Integrated structural safety analysis of San Francisco Master Gate in the Fortress of Almeida

Andrés Arce[1], Luís F. Ramos[1], Francisco M. Fernandes[2], Luis Javier Sánchez-Aparicio[3], Paulo B. Lourenço[1]

[1]ISISE, Department of Civil Engineering, University of Minho, Campus de Azurém, 4800-058 Guimarães, Portugal

[2]ISISE, Faculty of Engineering and Technologies, University of Lusiada Norte, Famalicão, Portugal

[3]Department of Land and Cartographic Engineering. University of Salamanca, High Polytechnic School of Avila, Hornos Caleros, 50, 05003, Avila (Spain)

E-mail: aarce.cr@gmail.com, lramos@civil.uminho.pt, francisco.fernandes@fam.ulusiada.pt, luisj@usal.es, pbl@civil.uminho.pt

Abstract – After more than three hundred years of being exposed to human and nature actions the Master Gate of San Francisco in Almeida, Portugal, has sustained visible extended damage. Although its importance, as a historical monument, is undeniable, no attempts have been done so far to determine its level of safety. In this paper several models are developed in order to achieve this goal. A brief description of the Gate's history is presented followed by a summary of the inspection and diagnosis procedures employed in this study and the results obtained from them. Later the type of numerical models selected are discussed as well as the methodologies used to represent damage. Finally results from the numerical models are presented in a first attempt to identify the safety level of this historic construction. Results indicate that although the structure has lost a great percentage of its original capacity is still safe.

Keywords – Non-Destructive tests, Geomatics, Finite element analysis; Historical construction;

1 Introduction

The cultural heritage industry provides jobs for more than 8.5 million people in the EU and up contributes to 4.5% to Europe's GDP (European Commission, 2016). On the other hand the cultural value of heritage can hardly be quantified. As an ancient military structure, the Gate of San Francisco in the Fortress of Almeida reminds us of Portugal's conflictive history in its search for independence. Ever since the creation of the Fortress of Almeida, the Gate of San Francisco has witnessed conflicts between Portugal and Spain and even survived the Napoleon's fierce attempts of invasion in 1810. This history attracts every year lots of tourists to visit the fortress of Almeida, especially the Gate of San Francisco. Therefore, it is of utter importance to understand the safety level and guarantee the stability of this monument to conserve its cultural value and guarantee the security of its visitors.

The Fortress of Almeida is a Bulwarked architectonical heritage that, although classified as Portuguese National Monument since 3rd February 1928, wishes to break barriers, clearing the path that leads to a global projection as a UNESCO World Heritage [1]. The desire of conservation of the heritage in Almeida is evident as not only part of the ruined heritage has been recovered, but also priority has been given to provide new life to these spaces, transforming them into museums, offices and diverse spaces for the benefit of the community. This determination was based on several initiatives: seminars, publication of the activities of the Center for the Study of Military Architecture of Almeida [2]; research works; protocols with universities and technical schools that have given shape, step by step, to a sense of sustainable safeguarding [1].

Previous researchers have developed an extensive campaign of inspection and diagnosis on two gates in the Fortress of Almeida, San Francisco and St. António gates [3], and the *Quartel das Esquadras* building [4]. From this compendium of investigations the work developed by Barros [3] based on several similar methodology [5] [6] [7] [8] was fundamental to study the structural condition as it focuses on the

inspection and diagnosis of the Fortress's Gates and comprehends an initial visual inspection with a photographic and damage survey, as well as a wide variety of in-situ and laboratory tests that determine the morphology of the structure and the properties of the materials. This investigation was essential for the later phase of modelling in which the structural level of safety is assessed. An example of this kind of approach is the FE modelling of the *Quartel das Esquadras* in the Fortress to evaluate the effects of a possible structural intervention [4]. Even though some parts of the fortress had already been modelled and analyzed this study is the first attempt of using computer modelling to assess the safety level of the Gate of San Francisco. This task was the focus of the present paper and it is justified due to the significant damage present on the stone masonry vaults, with lack of mortar joints and a severe deterioration process on going on the stone material. To foresee this objective, the paper followed a methodology with included historical survey of the fortress, inspection and diagnosis of the gate, definition of a modelling strategy, and a series of numerical safety analysis, with the simulation of the progressive deterioration process on the vaults (loss of material) by using phase analysis, including a sensitivity analysis of the effect of the structural parameters on the response of the structure.

It is of utmost importance to highlight that due to the intrinsic value of heritage buildings the techniques and technologies allowed for their study are highly restricted. The analysis of historical structures requires very advanced techniques that can obtain information without incurring on damage on the building. These techniques usually known as non-destructive techniques (NDTs) are the main tools used in this study. From the several NDTs used to study heritage buildings this study makes use mainly of laser scanning, georadar and sonic testing. Other authors have made great use of these aforementioned techniques in the assessment of structural stability of historical buildings. The case of study of the Cathedral Modena [9] in Italy is a great example. In this study laser scanning provided extremely valuable information that allowed to measure the different inclinations of masonry walls and pillars. This information combined to the understanding of the construction phases of the cathedral allowed to successive date the increases of

foundations settlements during centuries. Information that was then included in a non-linear phased structural analysis allowing a more complex and complete study and a better diagnosis of the structural stability of the cathedral. Another techniques utilized in this study is georadar. Georadar is of great use when is required to analyze the thickness of elements or morphology of them in cases where one of the sides is not accessible. This technique is used in this paper to study the morphology of the stone masonry walls and vaults and has been used for similar purposes in the investigation of historical buildings like the analysis of underground cellars in Toro (Zamora, Spain) where Georadar played a crucial role in understanding the thickness and morphology of vaulted elements and walls [10].

The paper is organized as follows. A first a brief description of the history of the Gate in the context of the fortress of Almeida is presented in section 2. Later the techniques and methods used for the inspection and diagnosis campaign are discussed in section 3. In section 4 a summary of the methodology approach chosen to create the model and properly quantify damage. The results are presented and discussed in section 5 in four subsections. The first subsection shows the response of the structure without damage through the application of a live load till failure, as an attempt to study the failure mechanism of the structure. In the second subsection a sensitive analysis is included to study their effect on the failure mechanisms. The following subsection consists in a phase analysis to study the evolution of the structure' response in time, subjected only to self-weight and with progressive loss of material since its construction. The last subsection includes the safety analysis by applying phase analysis in progressive induced damage and applying a live load till failure, simulating the effect of the current damage on the safety level of the Gate. The comparison between the results of the three sections shows the decrease in the ultimate live load as a consequence of the damage in the stone-masonry. Finally, the paper ends with the conclusions about the safety of the San Francisco Gate.

2 Description of the Fortress and the S. Francisco Gate

2.1 Historic Background

The Fortress of Almeida, composed of 6 bastions forming a star, is located in the heart of the historical city of Almeida near the city of Guarda, Portugal (Figure 1). Almeida is set on the east side of the Côa River, and due to its strategic location the city was condemned to be a place of war. In the middle age and till 1297 it was a space for dispute between Christians and Muslims. Later on, the city was a victim of constant sieges and attacks due to the conflictive climate that appeared after the independence from the Castilian Kingdom of Leon during the 13th century (Campos, 2009).

Figure 1. Aerial view of the Almeida fortress (Campos, 2009).

The fortress of Almeida has lived a very long life. Therefore it becomes relevant to describe its history in terms of construction, demolition and intervention phases that are shown in Figure 2**Erro! A origem da referência não foi encontrada.**. The timetable includes the history of construction since the first Muslim Castle, that would later become the Castle of Almeida, till the creation of a New Gate in 2006-2007, as compiled by the technical commission for the candidacy of Almeida as UNESCO world heritage [11].

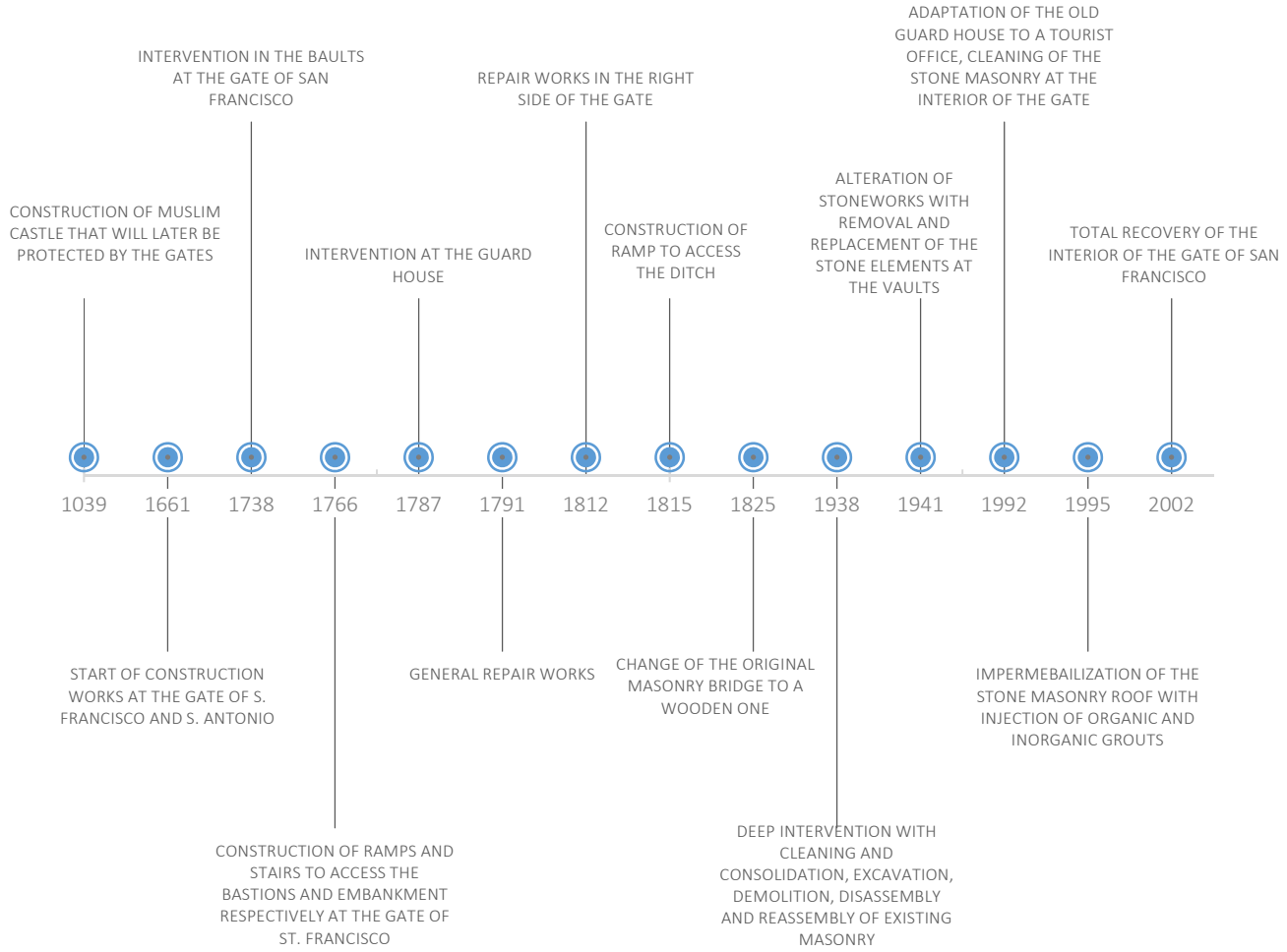

Figure 2. Timeline of interventions at the Gate of San Francisco

2.2 The Gate of San Francisco

The construction of the Gate of San Francisco began between 1661 and 1667. The geometry of the wall was thought in such a way that the inclination angle made projectiles bounce in the direction of the enemies, and the massive amount of earth acted as a cushion absorbing partially the impact of projectiles [11]. The structure is composed of two parts: the first is a curved tunnel allows transit into the city, and the second one is a lateral camera that was previously used as the house of the guard. This second section is considered to be added between 1744 and 1789. Also in this period, restoration works were done to replace damaged stones with new ones.

The French invasion in 1810 will pass down in history as the most destructive event both for the fortress and the Gate of San Francisco. The explosion of the gunpowder storehouse destroyed the castle and generated great damage to the fortress and specifically to the Gate of San Francisco. The bombing due to the siege did a huge contribution as well. By 1815 the order to start reconstruction works on the gate was issued but since the war was over in 1814 the urgency of reconstruction was low and the construction works were kept to a minimum. It was not till the 60's of the 20th century that a significant restoration project would take place. The Figure 3 shows the gate by that time. Notice the wide crack with deformations on the right picture.

Figure 3. State of damage in the Gate of San Francisco year 1962: at left the main facede with vertical cracks and loss of material; and at rigth a crack on the roofing system (stone roof).

In 1986, works continued in the San Francisco's Gate whose right side urgently needed consolidation and cleaning of the masonry. The mortar was then replaced for a hydrophobic mix with cement base. The mortar in this period had a proportion 1:2/3:6 cement, lime and sand [12]. The actual aspect of the Gate can be seen in Figure 4.

Figure 4. State of the Gate of San Francisco by 2016.

2.3 Structural Description for modelling

In the interior of the Gate two substructures can be differentiated: the tunnel that allows the transit out and into the city and the antique house of the guard whose purpose was to accommodate the guard of the Gate, but today is being used as a tourism office (Figure 5).

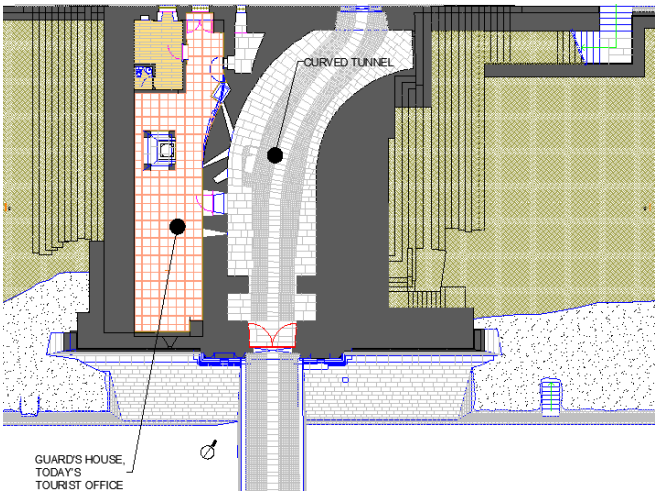

Figure 5. Plan distribution of the Gate of San Francisco

The supporting structure is composed by four main types of elements: arches, vaults, walls and lintels, all made of regular granite stone masonry with mortar joins as shown in Figure 6. The stone dimensions are, on average, in the order of 40 by 100 cm (side view).

Figure 6. Arrangement of granite stone masonry in the Gate of San Francisco.

Figure 7 shows the geometry arrangement of a cross section of the Gate of San Francisco. The main entrance consists of a curved barrel vault with perfect curved shape that has a diameter of 5.9 m at the entrance and it diminishes to 4.9 m on the opposite side. The transition of this geometry is smooth and the height is kept constant. To the left side of the tunnel there is another compartment constructed as the house of the guard. In this section another barrel vault acts as a roof and has the opposite geometrical evolution than the vault mentioned before. In this case the barrel starts with a diameter 4.5 m and opens to 5.9 m in the side of the interior of the fortress, and the height is also kept the same. The walls that sustain the barrel vaulted roof loads are respectively around 2.7 m high for the left vault and 3.7 m high for the right one, with a thickness varying from 1.60 to 1.70 m. According to the borescope camera survey and GPR tests, the vault thickness for the tunnel and the Guard's house was considered equal to 40 and 30 cm, respectively. The roof stone pavement was not modeled because it isn't part of the bearing system, being the weight substituted by a distributed load on the top of the filling material.

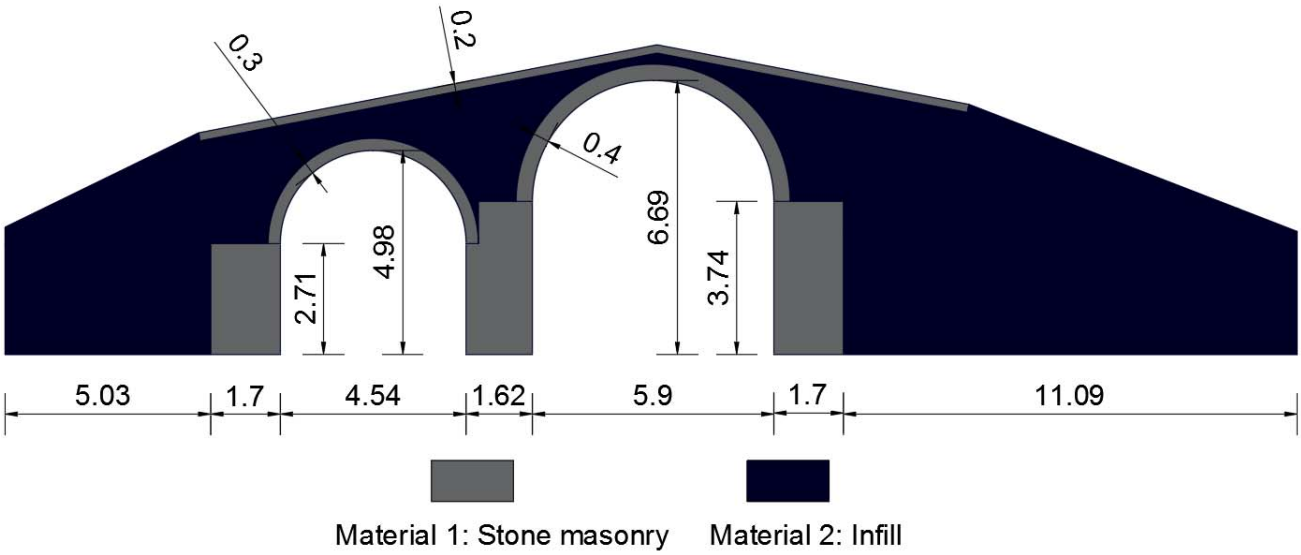

Figure 7. Transversal section of the gate with the assumed dimensions of the main structures and their material composition.

3 Inspection and Diagnosis

Traditional techniques, such as visual inspection, laboratory tests, and advanced nondestructive techniques (NDT) were applied to reach an overall understanding of the structural morphology and damage level. The mechanical properties were also estimated by the use of the most suitable techniques. In this case of study, NDTs are of the highest importance as some fundamental characteristics, for example the morphology and strength, needed to be determined without causing severe damage to the structure. Due to these requirements, sonic measurements were used for the mechanical assessment of the masonry and geomatics methods, namely Ground Penetrating Radar and Terrestrial Laser Scanner, were considered for morphology, damage and deformation assessment.

3.1 Nondestructive techniques applied in the study of the Gate of San Francisco

3.1.1 Terrestrial Laser Scanner

Terrestrial Laser Scanners (TLS) have nowadays a wide variety of sensors able to record complex objects in 3D, from digital cameras [13], to mobile laser scanners [14] or structure light approaches [15]. The

TLS has positioned as an attractive solution for the digitalization of architectural Heritage structures [13]. This sensor offers a wide range of advantages such as: (i) no dependency on specific lighting conditions; (ii) fast and accurate data acquisition; and (iii) high density of data, allowing the acquisition of millions of points in a short period of time. With the aim of creating an accurate numerical simulation and considering the complexity as well as the illumination conditions of the barrel vault, the TLS Faro Focus 120® was used (Table 1).

Figure 8. Terrestrial Laser Scanner used during the geometrical evlauation of the barrel vault.

Table 1. Technical specifications of the TLS Faro Focus 120®

Physical principle	**Phase shift**
Measurement range	0.6 – 120 m
Accuracy, nominal value at 25 m	2 mm
Beam divergence (mrad)	0.19
Capture rate (points/sec)	122 000 / 976 000
Spatial resolution at 10 m (mm)	6
Field of view	360º H x 320º V
Wavelength (nm)	905 / near infrared

Due to the size of the curved barrel vault evaluated (approximately 20.82 × 5.90 × 6.70 m^3) as well as the needed to record the damage areas, 5 stations were required. Each station was placed on an arbitrary local coordinate system, requiring the use of align procedures to place them into a common coordinate system. Considering this, the coarse to fine approach defined by Sánchez-Aparicio et al. [10] was used. Firstly a pair-wise registration was carried out, using for this purpose the Iterative Closest Point (ICP) algorithm [16] . Later, a global registration by means of the Generalized Procrustes Analysis (GPA) [17] was performed, throwing a registration error of 0.003 ± 0.003 m. As a result, a complete and dense 3D representation of the barrel vault was obtained (composed by 503 918 964 points) (Figure 9a and b).

Taking into account that the present point cloud will be used as the geometrical base for further numerical simulations, as well as the high amount of redundant data on the overlap areas, a decimation based on curvature was carried out [18]. As a result an optimized 3D representation of the barrel vault was obtained, made up by 9 301 121 points (1.84 % of the original point cloud) (Figure 9c) on which the areas near to the damage zones and joints are preserved.

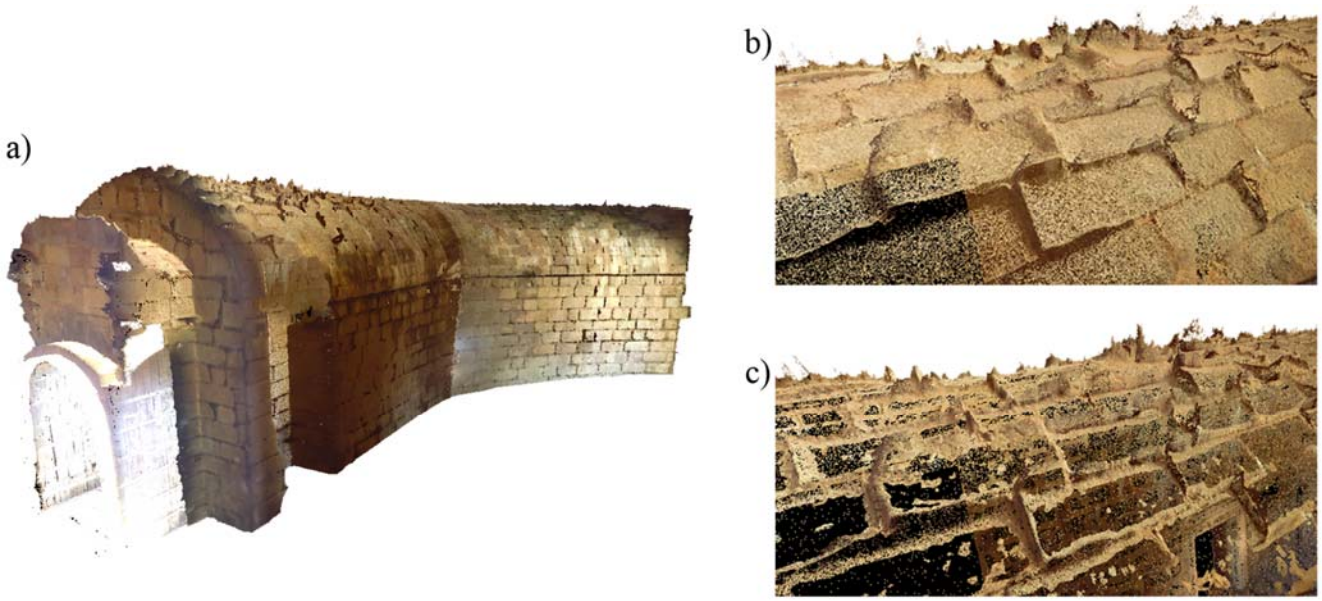

Figure 9. Point cloud obtained during the TLS campaign: (a) isometric view of the barrel vault; (b) detail at full resolution of the barrel vault; and (c) detail of the resampled vault point cloud.

3.1.2 Sonic Testing

The sonic testing campaign was based on indirect sonic tests that measure two type of waves: pressure or compressive waves "**P**" and superficial waves "**R**". During the execution of the sonic tests, the waves were created by means of an instrumented hammer connected to a computer. The computer measures exactly when the wave is created and a transducer (accelerometer) registers the resulted signal. Therefore the time it takes the wave to travel from its origin (location where the hammer hits) to its destination (location of the transducer) is known. Since the location of the hammer hit and the transducer are chosen by the investigator the distance the wave travels is known and therefore its speed as well.

Figure 10 shows the locations where indirect sonic tests were carried out. The sonic testing campaign included: 6 indirect tests inside the tunnel, plus 6 indirect tests at the stone masonry roof. For each test, the velocity of the waves was measured an average of 8 times. Every time the stone was hit in the same location. The corresponding velocity reported for each test was calculated as an average of all measurements of velocity for every location.

Results for sonic tests are provided in Section 3.3. Locations A, F and G refer to tests in which the sonic wave passed through both stone and mortar joints thus giving a value that is representative for the stone masonry composite. Tests from locations D, E, and C refer to the wave velocities traveling solely through stone.

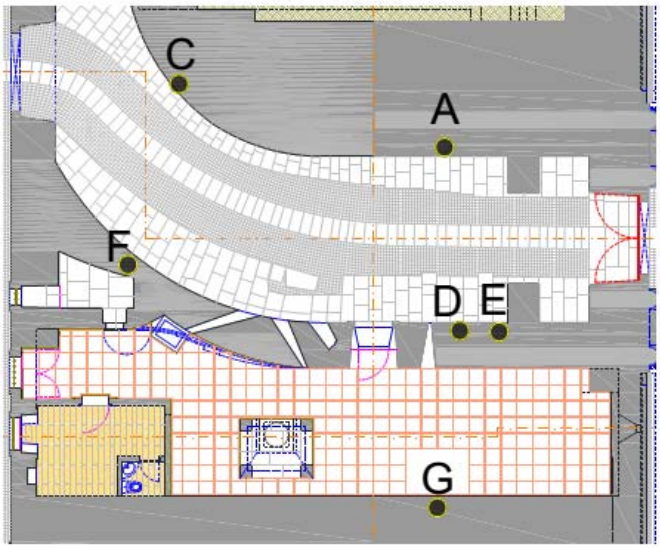

Figure 10. Location of indirect sonic tests,points A, F and G refer to tests on stone masonry; C. D, E and G refer to tests on stone only.

3.1.3 Ground Penetrating Radar

Ground Penetrating Radar was used with the objective of obtaining information about the internal morphology of the walls, as well as values for the thickness of the vault of the barrel vault. The equipment was the RAMAC/GPR from Mala Geosciences, Inc®. Due to the thickness of the stone parameters and the depth at which some of the elements were located, two antennas with 500 and 800 MHz of central frequency were used. Figure 11 illustrates the locations where the tests were carried out along the internal walls, to gather information about the thickness and constitution, and over the roof, to estimate the value of the vault thickness and nature of the infill. The results are presented in Section 3.4.

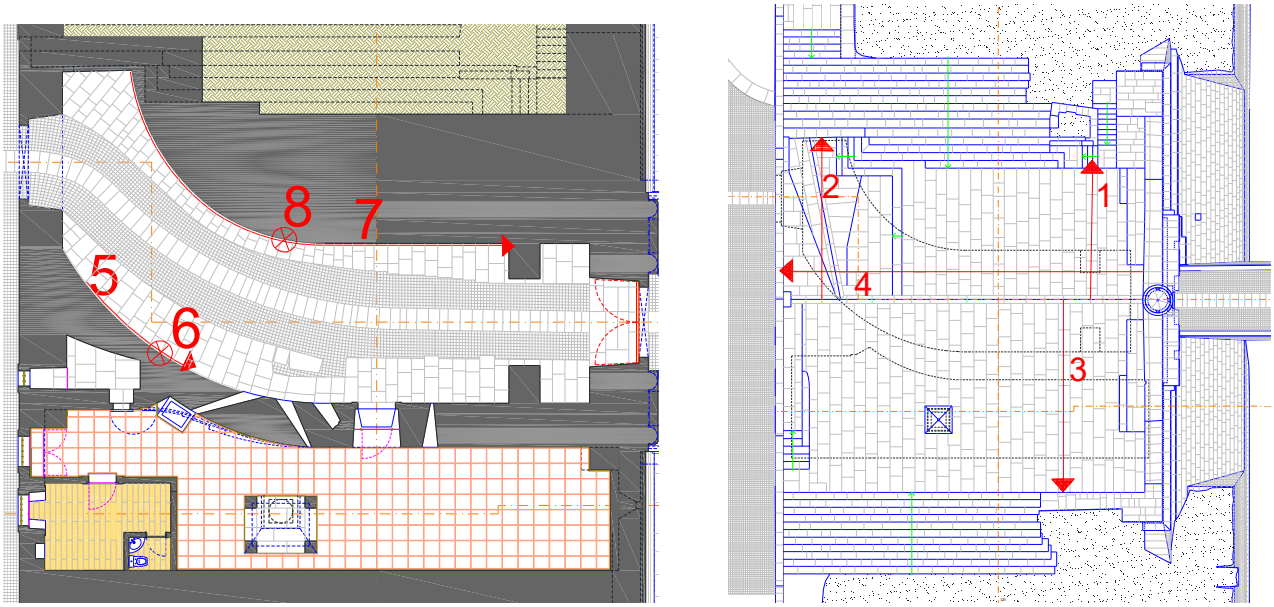

Figure 11. Location of the goeradar tests: along the internal walls and over the roof of the tunnel.

3.2 Assessment of damage

3.2.1 Identification of problems in the Visual inspection

Visual inspection allowed to identify numerous pathologies both structural and nonstructural. In the nonstructural category the presence of lichens were identified, being part of the "Nitrofilos" family, a species that benefits from deposits of nitrogen and dust to grow (Barros, 2016). It is very likely that this lichens benefit from the nitrogen that is carried out of the soil fillin the walls and that is probably washed out by infiltrated water. Vegetation growth was also identified. Additionally, the loss of superficial material in the granite stones, humidity stains and the presence of salts at the stones surface inside the transit tunnel were observed (Figure 12).

Figure 12. Non structural afectations in the Master Gate of San Francisco: a) lichen attack; b) spalling of the granite stones; and c) humidity stains.

The main structural concerns are the great loss of material in the joints (Figure 13) and the loss of material in the granite blocks used for the stone masonry. Material erosion could be related to a combination of the presence of salts and water.

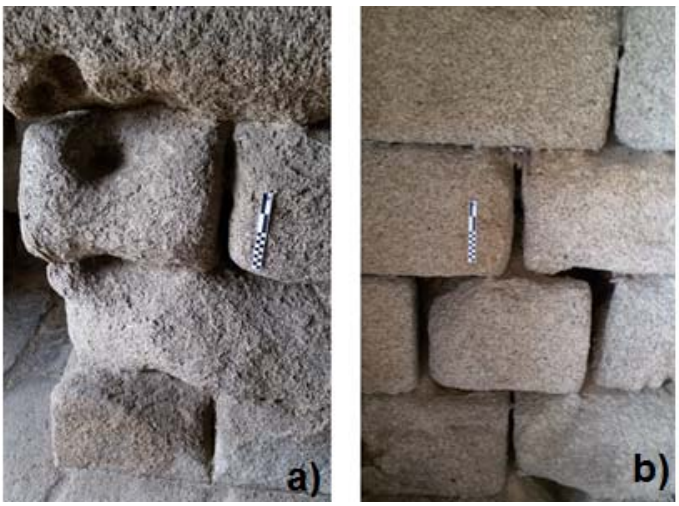

Figure 13. Deep degradation of granite stones and loss of the mortar in joints: a) at the base of the wall; and b) on the intrados of the vault.

3.2.2 Identification of location and level of damage based on TLS

The loss of material in the joints between the voussoir stones seems severe, according with the results provided by the TLS point cloud (Figure 9). A number of 28 2D sections extended through the tunnel depicts precisely the loss of material in each joint (Figure 14a). The profiles from the area close to the

entrance of the gate (zone A in red) showed the highest level of deterioration and therefore were selected for the further numerical analysis (Figure 14b). In this area, the damage is characterize by the loss of the material but also by the alignment in plane of the joints with higher level of deterioration, which increases the risk of failure. Figure 14c shows a superposition of the cloud of point 2D profiles in Zone A which then would be used as a base for modelling the damage in the structure.

a)

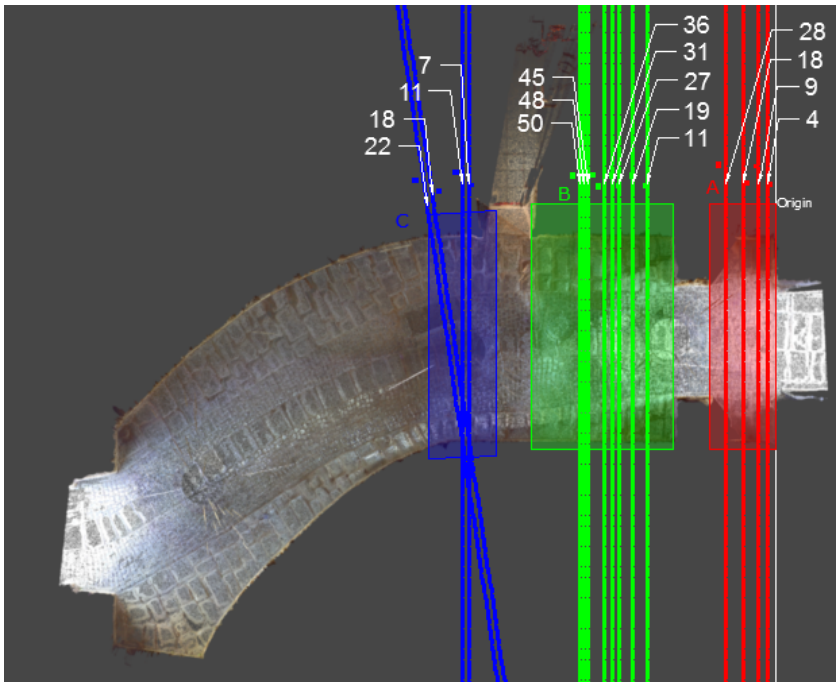

b)

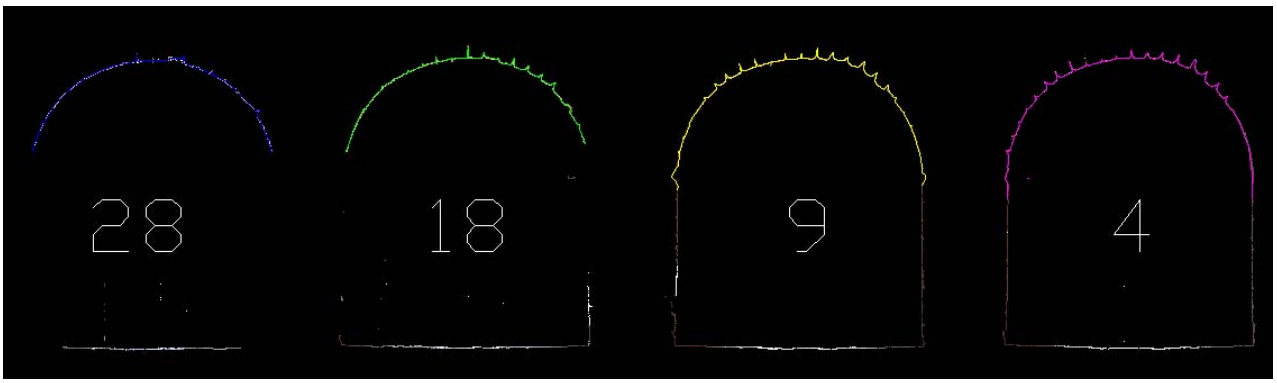

c) 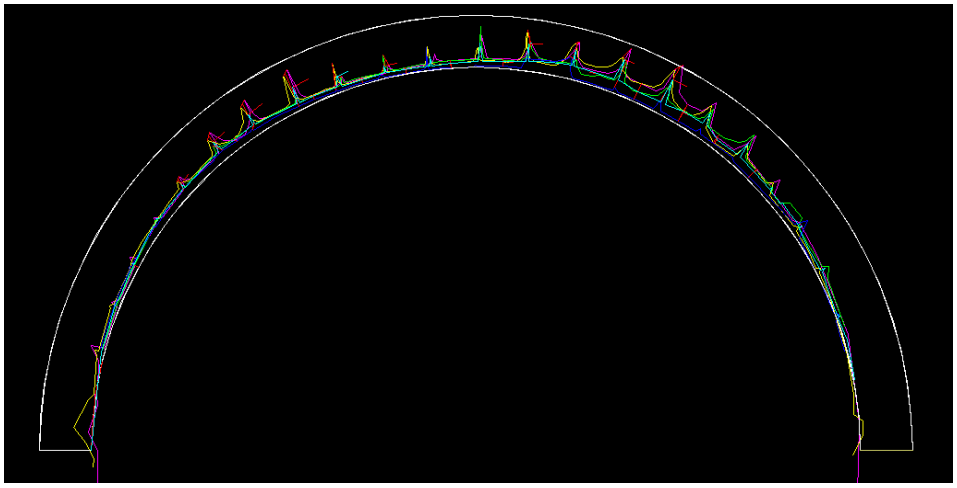

Figure 14. a) Laser scanning testing zones A (Red), B (Green), C (Blue). b) Damage profiles from clouds of points for Zone A c) Superposition of the most damaged profiles and resultant vault considered for the numerical simulations.

3.3 Mechanical properties as obtained from the Sonic Testing

The results of the sonic test are presented in Table 2. The average compressional wave traveling through the stones ($\boldsymbol{V_P}$) was equal to 1851 m/s with a coefficient of Variation (CoV) equal to 5%. The obtained value is lower when compared with the results for sound granite stones [19] [20], meaning that the stones can be deteriorated due to the presence of salts. In terms of the masonry results, the average velocity was equal to 1598 m/s with a CoV of 14%. It should be stressed that the velocity of the sonic waves on the masonry material (crossing the mortar joints) is very close to the values obtained from the stones, indicating the less impact on the mortar joints in the results, emphasizing the idea of deteriorated stones. The ratio between $\boldsymbol{V_R}$ (average velocity of **R** waves) and $\boldsymbol{V_P}$ velocities for stones and masonry material was equal to 0.50.

Table 2. Sonic wave velocity results of indirect sonic tests applied in the stone masonry components in the San Francisco Gate.

Indirect tests	Distance (cm)	V_P (m/s)	V_R (m/s)	V_P / V_R
Point A (stone)	100	1986	987	2.01
Point C (stone)	70	1828	906	2.02
Point D (stone)	90	1819	854	2.13
Point E (stone)	130	1772	976	1.82
Average	-	1851	931	1.99
CoV	-	5%	7%	7%
Point A (masonry)	70	1517	778	1.95
Point F (masonry)	100	1431	738	1.94
Point G (masonry)	0.9	1847	870	2.12
Average	-	1598	795	2.00
CoV	-	14%	9%	5%

The values of V_R and V_P velocities were then used to obtain the dynamic modulus of elasticity and poison ratio based on the same procedure used by Miranda et al [21]:

$$\frac{V_p}{V_R} = \sqrt{\frac{2(1-v)}{(1-2v)} \frac{(1+v)^2}{(0.87+1.12v)^2}} \qquad \text{Equation 1}$$

$$V_P = \sqrt{\frac{E}{\rho} \frac{1-v}{(1+v)(1-2v)}} \qquad \text{Equation 2}$$

Where V_p is the velocity of the P wave in $\frac{m}{s}$; V_R is the velocity of the R wave in $\frac{m}{s}$, ρ is the density of the material, v the Poisson modulus and E the young modulus.

As it can be seen from the equations 1 and 2, the density ρ is a property that must be known prior to the calculation of the Young modulus. Density of the stone masonry varied from 1900 kg/m^3 to 2400 kg/m^3. This variation was expected as some sections are more weathered than others thus resulting in affected areas with less density. The values of ; V_R and V_p derived from the sonic test campaign were used to calculate the poisson ration v according to equation 1. After calculation of v, equation 2 was used to calculate the Young modulus E. The process was repeated for the two extreme values of density mentioned before, thus two vlues of E were obatained. The final value of E chosen was calculated as an average of the two values of E calculated in the previous step

Since the obtained Young's modulus corresponds to the dynamic one, for further analysis it was considered that the static Young's modulus was equal to 70% for the case of the masonry work. The latest reduction, tries to take into account the morphology of the walls and the fact that the sonic tests were carried out at the surface of the walls.

3.4 Geometry and morphology identification based on GPR

Figure 15 illustrates two radargrams that resulted from the survey to the vault and to the masonry walls along the tunnel. The inspection of the vault resulted in an average thickness around 35 to 45 cm. The wall survey showed the first parament of an irregular masonry multi-leaf wall. This first leaf exhibits an average thickness of 40 cm, although the thickness should be much larger, up to 1 m, as indicated in the last part of the radargram Figure 15b and c.

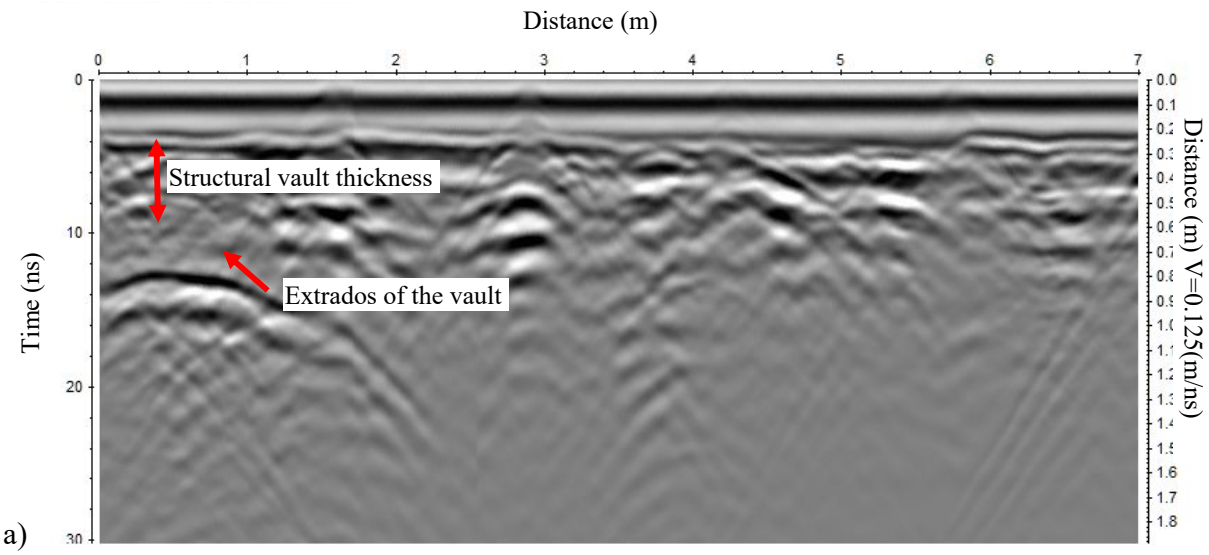

a)

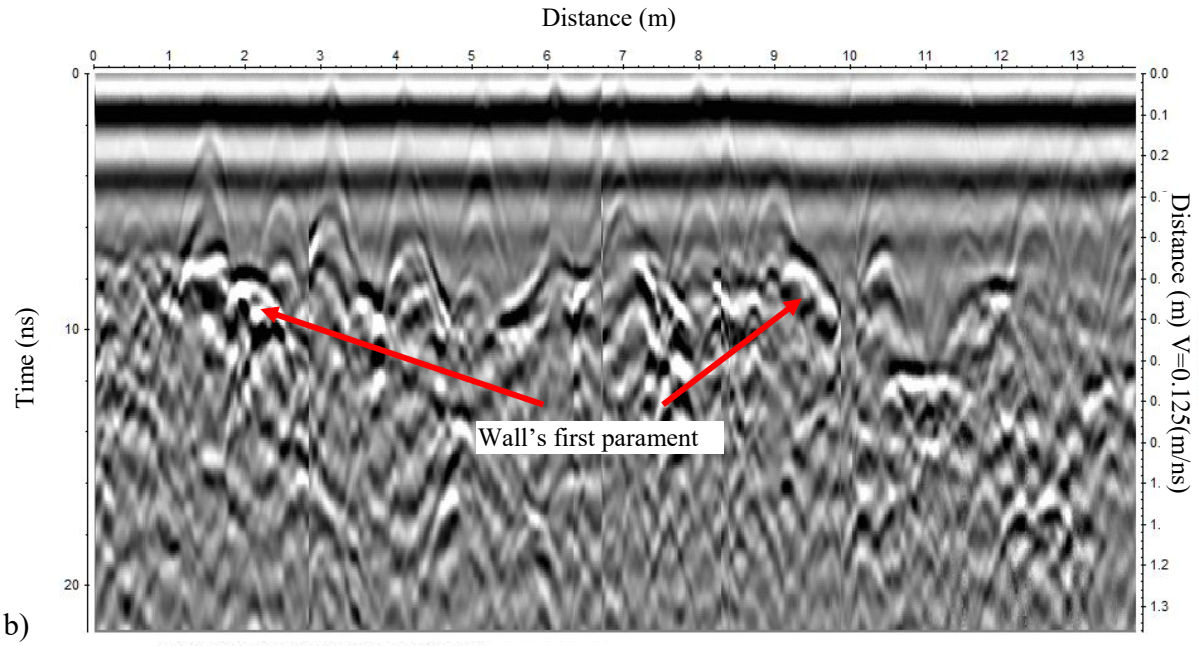

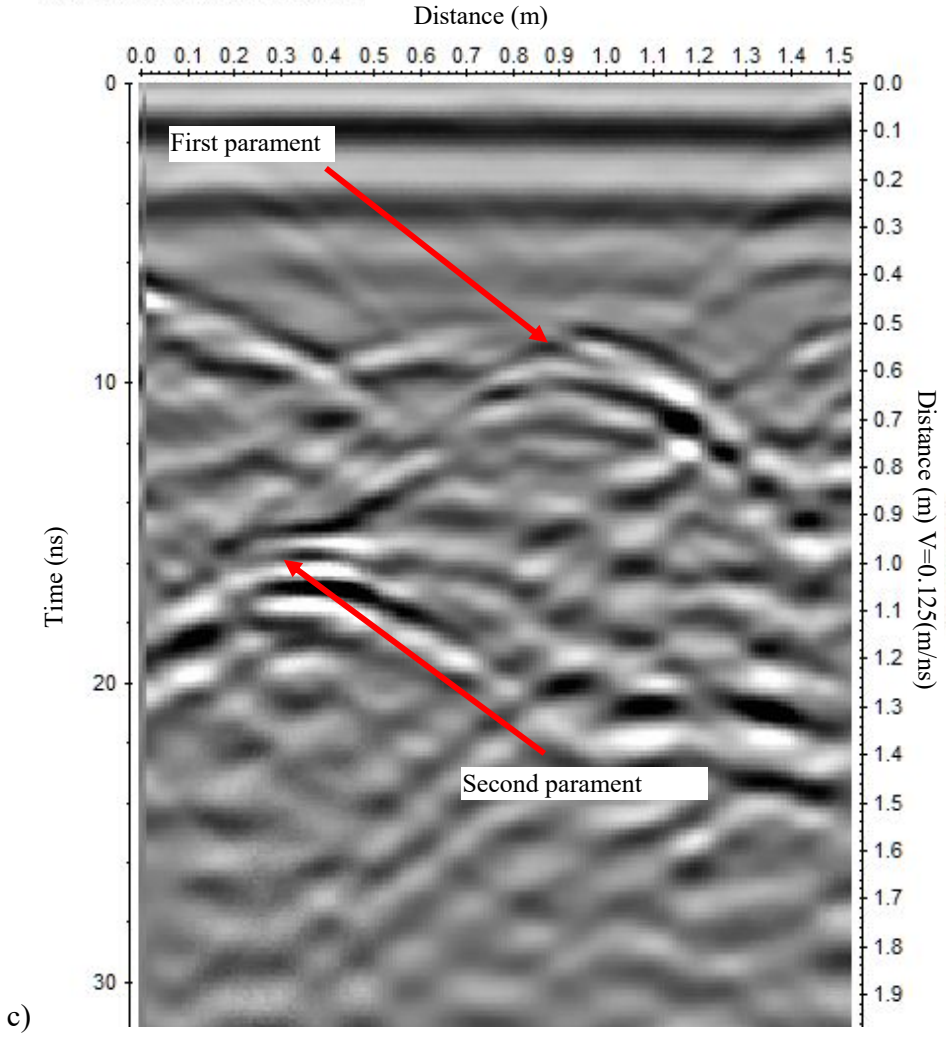

Figure 15. Radargrams illustrating the charaterization of the vault (a) and the masonry walls with horizontal (b) and vertical (c) profiles.

4 Modeling Procedures

4.1 Macro Modelling approach

A macro model analysis was chosen for this study. Since this method requires the assumption of the stone and joints to act as a unique and homogenous material [22] [23] it has the disadvantage that the material properties become harder to obtain in a precise way. Therefore a sensitivity analysis was implemented to overcome this limitation. Additionally, due to the inherent nonlinearity of masonry and, globally, all materials used in old masonry structures, a nonlinear analysis was used to consider the possible nonlinear physical behavior of the structure. It is important to remark that this investigation focuses on the study of evolution of damage in the structure due to the loss of material in time. The present document intends to study the evolution of damage in the Gate of S. Francisco due to the loss of material in the joints and stone, no dynamic analysis was part of this study. Almeida is located in seismic zone 1.6. This zone has the lowest possible value of seismic acceleration according to the Portuguese national annex to the euro code $0.35\frac{m}{s^2}$ [24]. Besides this, the structure posse a geometry in which the center of gravity is evidently located in the lower part thus making a seismic analysis less critical in comparison to the evident deep damage in the joints of the masonry vaults.

The numerical analysis was carried out using two software packages: DIANA 9.6 [25] for processing and Midas Fx [26] for pre and post processing. Since the structure has a tunnel typology, the dimension out-of-plane can be considered to be much larger than the in plane dimensions, restraining thus out of plane deformations (plain strain problem). Therefore it was preferred for this study to create a 2D model based on the most damaged cross section in the tunnel. Figure 16 shows the model's full mesh. Notice a higher refinement of the mesh in the right vault as it became necessary as to be able to appropriately incorporate the damage in the model. This consideration will be further explained ahead.

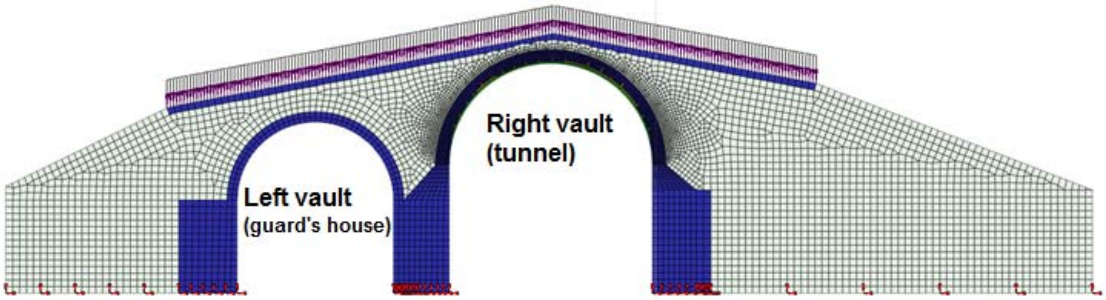

Figure 16. Plain strain model of the Gate of San Francisco.

Regular plain strains elements were used for nonlinear cracking available on DIANA software [27]. From the family of regular elements two are preferred: CT12E – triangle, 6 nodes, and CQ16E – quadrilateral, 8 nodes. Both elements use quadratic interpolation, Figure 17. Finally, two load configurations were implemented: self-weight only and self-weight combined with a live load of 5 kN/m^2, which was applied as a distributed linear load on the roof of the structure (see Figure 16).

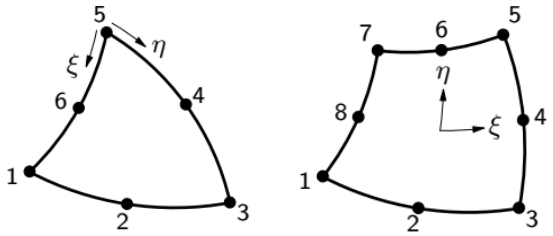

Figure 17. Element selection for non linear analysis [27].

4.2 Constitutive law and material properties

The constitutive model chosen is the Total Strain Crack Model that follows a smeared approach for the fracture energy. The strain concept selected was the Rotating Crack model in which the stress-strain relationships are evaluated in the principal directions of the strain vector. Under this configuration the material can present cracking or crushing in the loading process [27]. For this model the tensile behavior was represented by an exponential curve and the compressive by a parabolic one. Table 3 shows a

compilation of material properties for the model. Stone masonry properties from literature are also included. The last columns show the values for stone masonry derived from the elastic wave tests and the values chosen for the infill material.

Table 3. Parameters for materials according to literature review and testing campaign.

Mechanical Parameters	Masonry walls				Estimated/Assumed	
	Lourenco et al. [23]	Núñez-García [4]	Garcia-Roca [28]	Lança et al. [29]	Stone-masonry	Infill
E (GPa)	3	2.06	3	3	2.54	0.50
ν	0.20	0.20	0.20	-	0.25	0.20
ρ (kg/m^3)	2300	2200	2000	2200	2100	1900
f_c (MPa)	3 to 6	2.0	6.0	3 to 9	2.4	0.5
G_c (N/m)	1.6 × f_c	3.2	9.6	1.6 × f_c	3840	800
f_t (MPa)	0.00	0.2	0.10	0.0	0.12	0.025
G_t(N/m)	0	120	50	0	120	25

4.3 Meshing refinement and damage modelling

Two scenarios were considered in this study: (i) the original state; and (ii) the actual deteriorated state. The reason behind this dual study is to allow for comparison of the original an actual state, therefore, understand the effect that weathering has taken on this structure. The first scenario (original state) represents the geometry of the structure after construction without any damage in the joints and includes all elements that exist in the mesh. A second scenario was created by removing elements from the mesh in the same places where the higher loss of material was observed. The elements removed are meant to represent the loss of material in the both on joints and voussoir stones. The removal process was developed in three phases, allowing for the state of stresses to be redistributed after each step.

Figure 18a shows the mesh refinement in the vault over the entrance, while Figure 18 b, c and d show the step by step removal of elements till the actual level of damage (last step), this same picture includes the 2D diagram representing the damage according to the TLS survey presented in Section 3.1.1. Notice how the mesh has been accommodated to follow, as truth as possible, the line of damage in the vault.

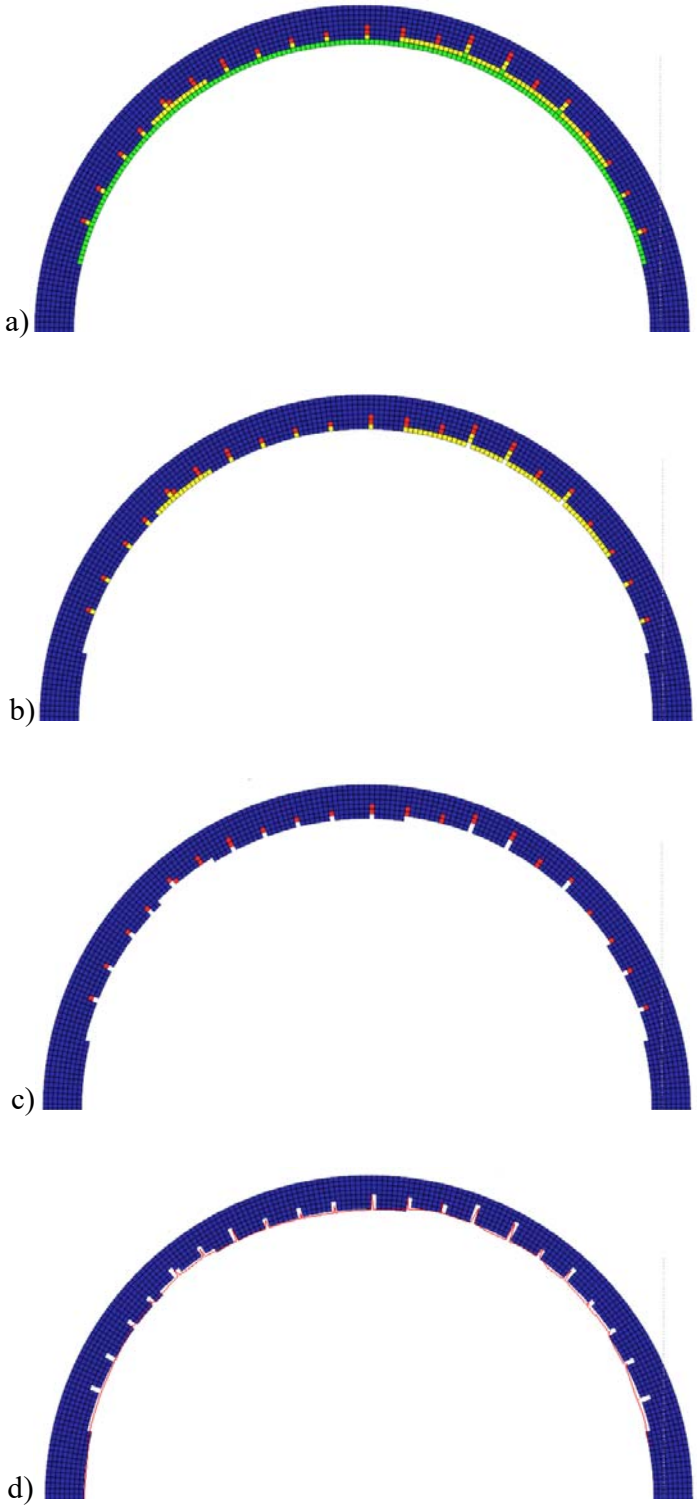

Figure 18. Refinement of the mesh in the right vault: a) Complete mesh for the right vault; b) Mesh after the removal of the first group of elements; c) Mesh after the removal of the second group; and d) Removal of all non exixting elements and actual state of deterioration of the vault.

5 Results and discussion

5.1 Analysis of the original structural condition

For the analysis of the original structural condition the self-weight was totally applied in four steps before initiating the application of the live load incremented 1.25 kN/m^2 per step. To control the linear/nonlinear behavior of the structure due to the live load increment, a single control point was chosen. The control point is located in the intrados of the biggest arch, corresponding to the area of highest deformation of the structure as a result of the applied load.

Figure 19 shows the displacement of the control point against the live load factor. The nonlinear behavior starts to be evident when the load factor reaches the value 30 (100% of the self-weight and a live load of 150 kN/m^2). From this point, the structure shows a non-linear behavior until failure, at load factor equal 49 times the live load (100% of the self-weight and a live load of 245 kN/m^2).

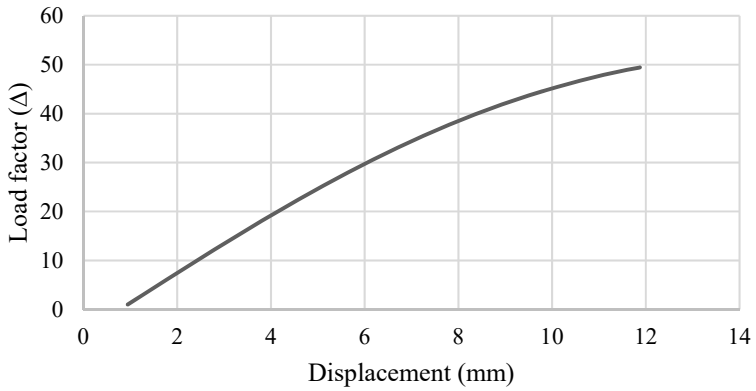

Figure 19. Load displacement diagram of the original structure for incremental of live load

Local failure occurs in the structure by the collapse of the right barrel vault in which five hinges are formed before failure. Results from crack pattern analysis clearly show a severe damage in the middle of the intrados of the vault (Figure 20a). This effect, combined with the crushing of material by compression on the sides (as seen in the blue areas in Figure 20b) results in excessive deformation in the vault and the

generation of a local mechanism of failure. At failure, the compressive stresses have reached the maximum value of the material capacity, i.e., 2.4 MPa. So in this case, the stone masonry material that composes the supporting structure reaches the limit capacity in the right vault, specifically in the base of the vault as it is depicted by the blue colored zone in Figure 20b. The failure mechanism is reached by crushing of the material in the base of the vaults without producing important damage at the base of the columns.

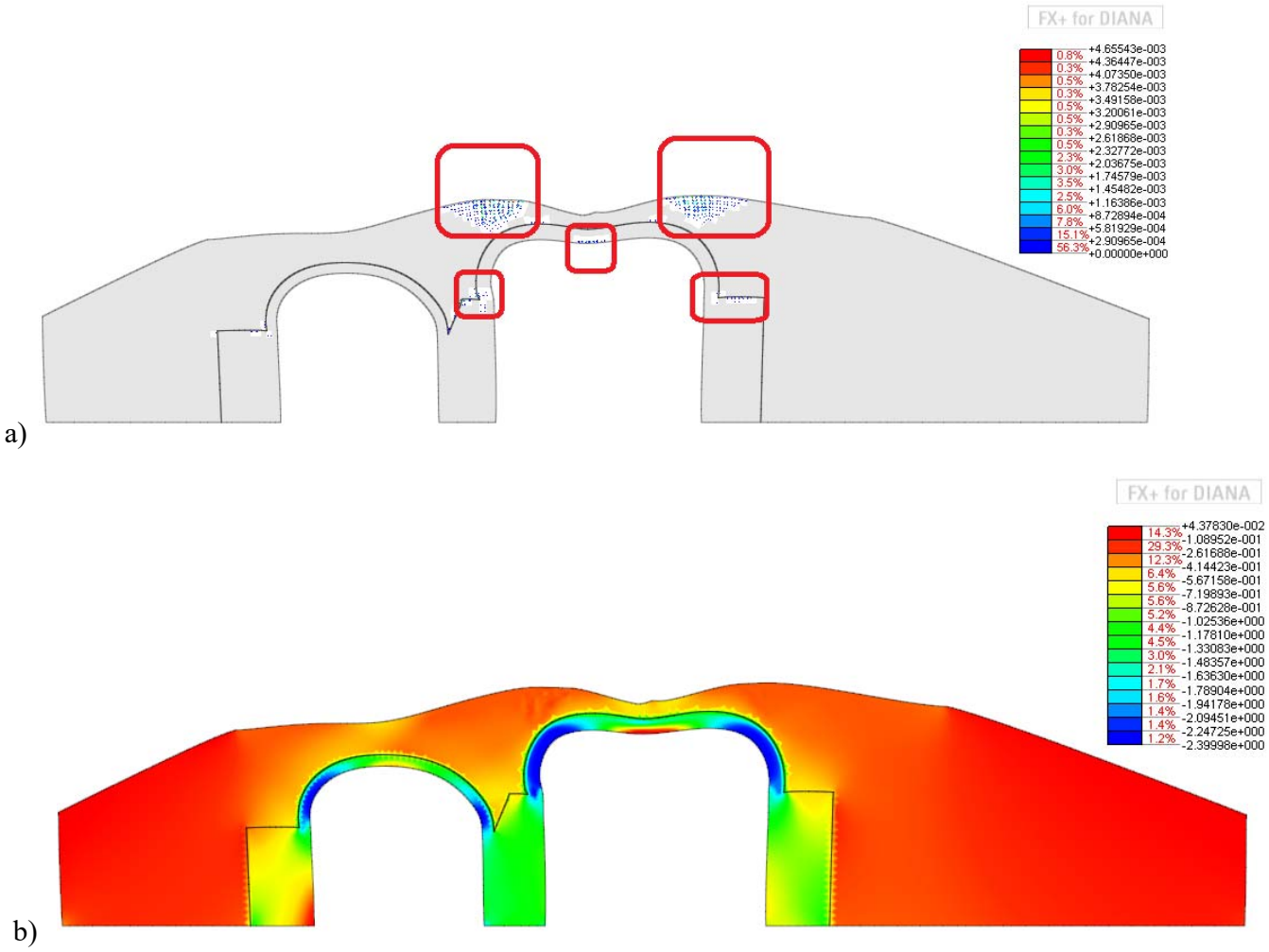

Figure 20. Structural response to an ultimate live load of 245 kN/m a) Crack locations b) Principal compressive stress [MPa].

5.2 Sensitivity analysis

As seen in previous section, the compressive material parameters were predominant and responsible for the failure of the structure. But due to the uncertainties on the estimation of all material properties and to fully understand its importance on the structural response, a sensitivity analysis was carried out by varying the compressive strength, the tensile strength, and the Young modulus of the masonry vault. In the analysis the assumed values for the selected parameters presented in Table 3 where multiplied by a factor of 2 and 0.5. Concerning the fracture energy, a proportional reduction to the strength was considered in compression and in tensile behavior.

Figure 12 presents the overall influence of the different parameters: compressive capacity, tensile capacity and modulus of elasticity. Notice in Figure 21a how the response of the structure is almost directly proportional to the variation of the compressive strength (and fracture energy) limit of the stone masonry. Duplication of the compressive strength parameter results in an increase in the load factor from 49 to 74 (≈ +50%). A reduction from 49 to 26 (≈ –50%) is obtained when the same property was halved.

Concerning the variation of the tensile strength (and fracture energy) of the material, its influence does not show any relevant effect in the failure history of the material as shown in Figure 21b. For the reference properties the first crack appears in the middle of the intrados at load factor of 11.8, while it develops much earlier at load factor 2.97 for half the tensile strength. Duplication of the tensile capacity resulted in a later observation of cracks, at load factor 29.6. Even though the comparison of history of crack apparition shows that the tensile strength does have a high influence in the formation of cracks, this effect is not reflected in the load history of the whole structure. This result can be interpreted as that the damage in tension is highly smaller than the one in compression. Therefore the structure failure is mainly governed by crushing of the material in compression.

The influence of the Young modulus of the masonry vault is shown in Figure 21c. The results presents a direct change in the slope of the material curves in the load versus displacement diagrams. It is clear that a duplication of the modulus of elasticity results in a higher stiffness as the slope of the curve becomes higher. The structures rigidity is as well diminished after its modulus of elasticity its cut half. It must be noted that, while changing this parameter, the modulus of elasticity of the infill was not altered, which again point out the relevance of the material properties of the stone masonry structure compared to the infill material properties.

The last sensitivity analysis was devoted to the influence of the soil infill material. The variation of the infill from a nonlinear material to an elastic one did not have a significant impact on the maximum load that the structure could take. The ultimate load factor varied from 49 to 56, which did not represent a large influence relatively to the impact of the variation of properties of the stone masonry. The crack pattern remained the same in the supporting structure while no cracks appear in the infill (see Figure 22a). Second, a different constitutive law was used for the soil using a Mohr-coulomb rule (soil model), where the cohesion was considered equal to 200 kPa, the tangent of friction angle was equal to 61.6º, the same value for the dilatancy angle, and a cap tensile strength equal to 0.02 MPa. For this model, the load factor significant decreases, showing high influence of the soil properties. Figure 22b shows a comparison of the structure's behavior as a result of a change in the infill model. The nonlinear infill modeled with a total strain crack model results in a general higher stiffness for the structure and a higher load factor when compared to the soil model. A value of 49 compared to a value of 18.1. The soil model shows a more clear mechanism of failure (see Figure 22b) which seems to make it a more adequate candidate to use for the study of the structural behavior of the Gate of San Francisco. But there is no certainty of what kind of material is in the infill as there are records that show there have been grout injections in the past.

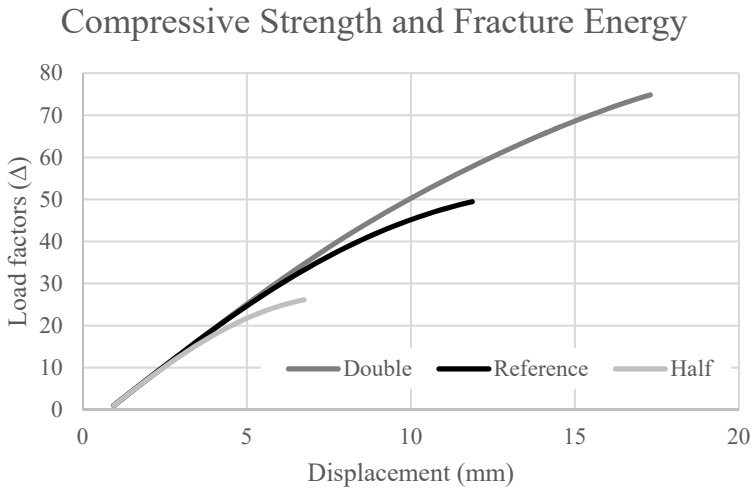

a)

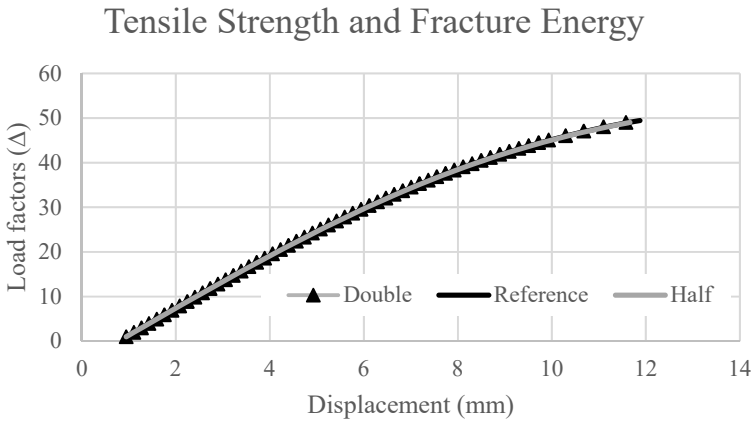

b)

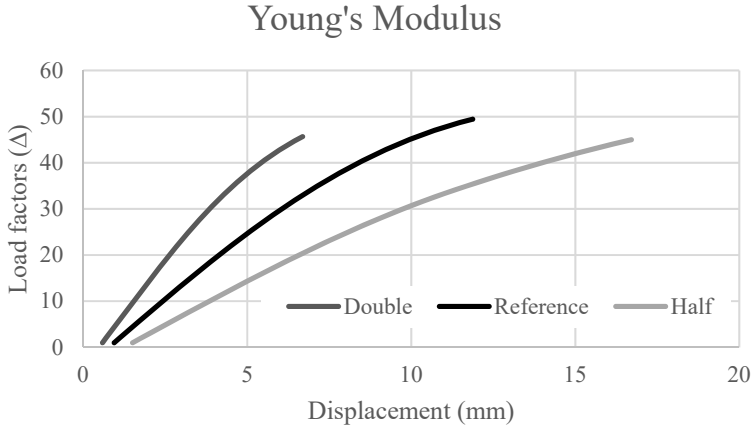

c)

Figure 21.Load vs. displacements curves as a result of a variation in the following parameters: a) compressive capacity; b tensile capacity and c) Modulus of elasticity.

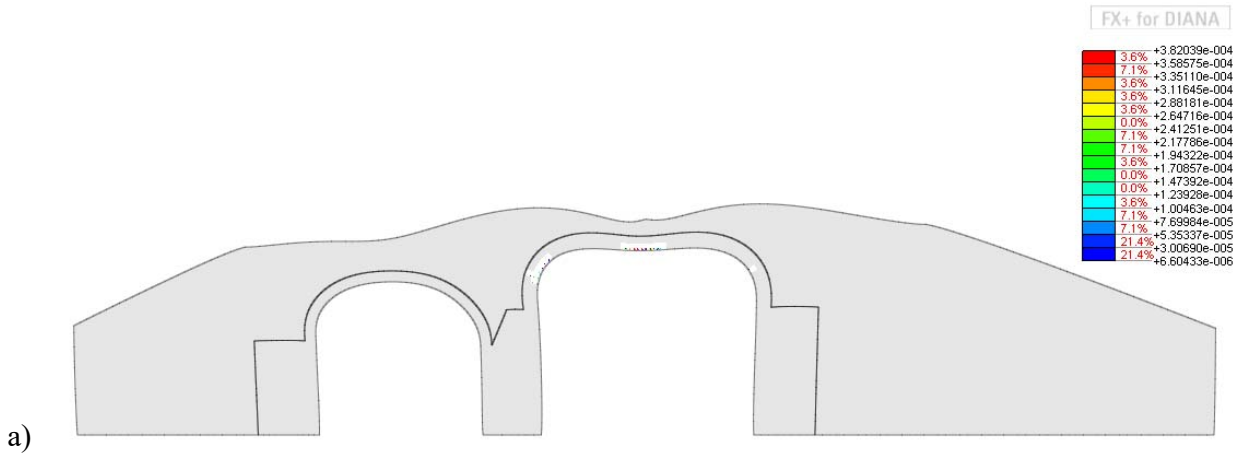

a)

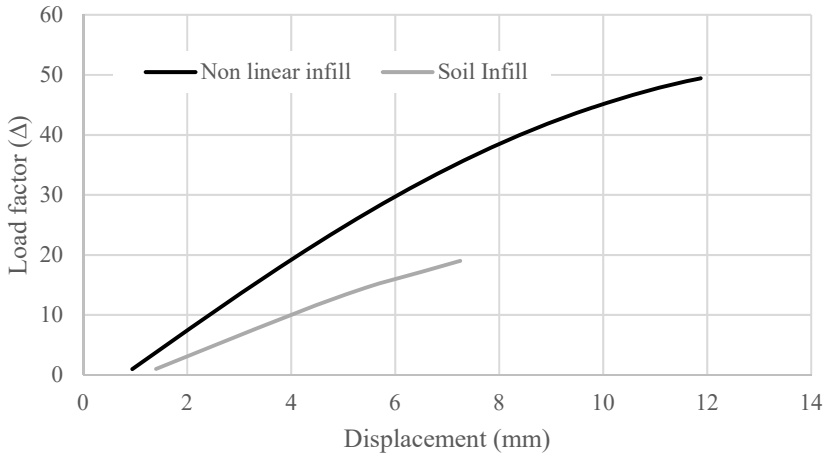

b)

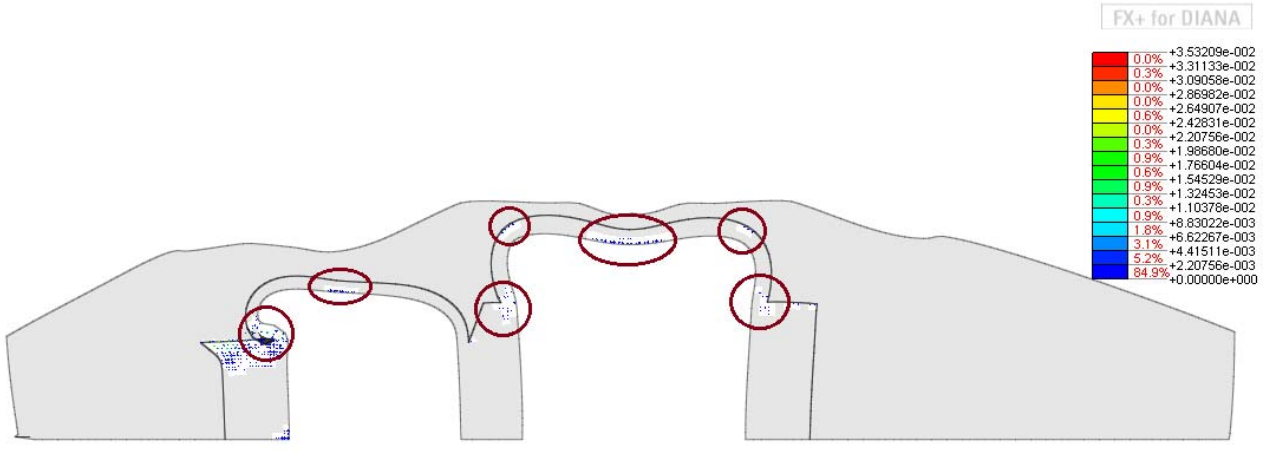

c)

Figure 22. Sensitivity analysis for the soil infill: a) Crack pattern for elastic infill at the maximum live load factor; b) Comparison of load vs. displacement for a soil infill; and c) Crack pattern for a model with a soil model for the infill.

5.3 Analysis of the damage condition

The study of the evolution of damage in the structure was first performed solely under the effect of self-weight. With the intention to replicate the actual evolution of stresses in time. The analysis starts with the model reproduction of the original structure (Phase 0) where only the self-weight load was applied. Subsequently the actual state of deterioration was considered in three phases described as: Phase 1, Phase 2 and Phase 3. The way damage is taken into account in the model is by the removal of elements which emulates the actual loss of material in the mortar joints and in the stones. The groups of elements which were removed in each phase were previously identified in Figure 18. Following the removal of elements, a stress redistribution takes place. The change of stress in each phase is a consequence only of the redistribution of stresses as no new loads are added to the model in these scenarios. Table 4 summarizes the results from this study. All maximus were found in the right vault. In all cases the stress state in compression does not even reach a quarter of the material's capacity for this property. The values of tension after the third phase show that the level of principal stress in tension is close to the material's limit capacity and explain the appearance of cracks in location. Maximum vertical displacement was measured in the middle of the right arch.

Table 4. Summary of evolution in time of the structural properties from zero to the actual state of damage.

Phase	Maximum displacement (mm)	Maximum principal compressive stress (MPa)	Maximum principal compressive strain (mε)	Maximum principal tensile stress (MPa)	Maximum principal tensile strain (mε)
Phase 0	0.79	0.41	0.16	0.06	0.45
Phase 1	0.84	0.45	0.17	0.06	0.49
Phase 2	0.91	0.59	0.21	0.12	0.50
Phase 3	0.98	0.58	0.21	0.11	0.57

Next, another phase analysis considering the self-weight adding the live load was carried out. In this analysis, the elements that existed in the original structure were removed until the geometry of the model corresponds to the present state of the structure. In the first scenario the structure is loaded its self-weight and only one group of elements is removed before applying the live load till failure. In the second scenario the self-weight is applied and later two groups of elements are removed in two consecutive phases, before applying the external live load till failure. A last third case repeats the procedure but involves the removal of three groups of elements that represent all the material that has been lost since the structure was constructed. As well as in the previous analysis the groups of elements removed are shown in Figure 18 section 4.3.

The first step implies the removal of the most exterior layer of elements in the intrados of the vault (Figure 18b). This results in a higher concentration of compressive stresses in the vault and a general reduction of the maximum load the structure can resist. Load factor decreases from 49.0 to 40.1 (Figure 26), which represents around 20% of loss in the structure's ultimate capacity due to a general loss of material of 5 cm in the intrados of the vault (12.5% of the thickness). Figure 23 shows the compressive zones in the base of the vault where the crushing of the material occurs. Note that the compressed zones are not focalized but evenly distributed along the intrados base of the vault.

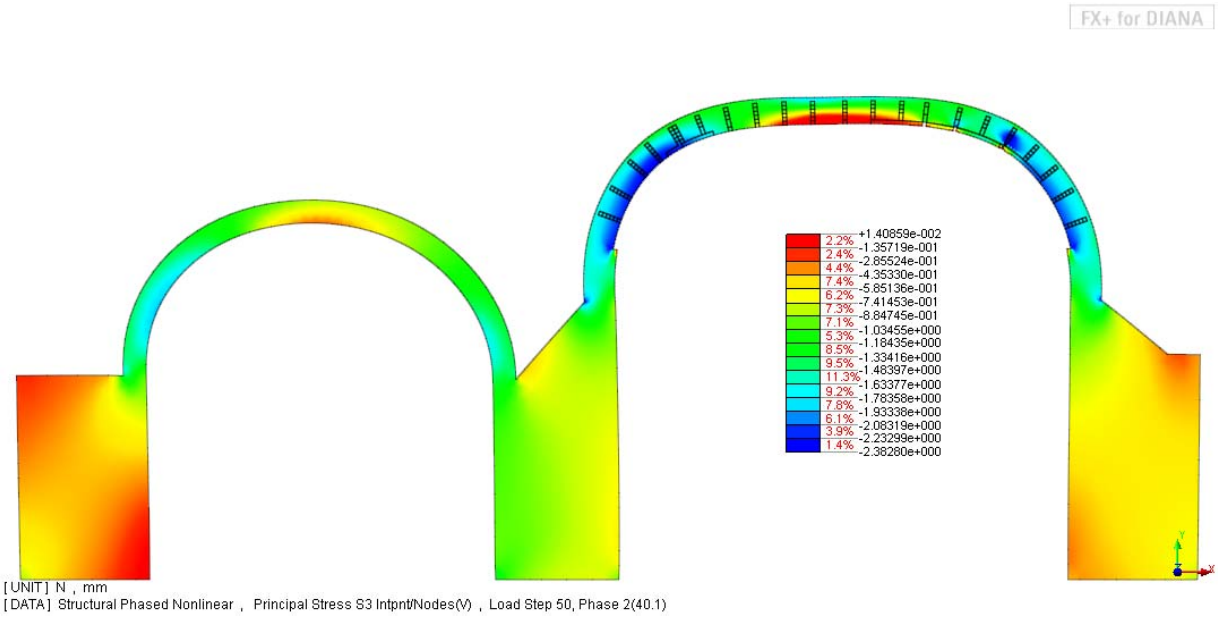

Figure 23. Principal stress σ3 for symmetrical live load Phase 1 [MPa]

By removing the second section of elements (Figure 18c), the ultimate factor lowers a total of 40%. Almost half the capacity of the structure has been lost at this stage and this model does not even represent the current level of damage. Anyway the load factor has lowered to 29.2 which is still extremely high, indicating that even though half the capacity has been lost the structure is still safe. Figure 24 shows the principal compressive stresses for this load factor. The biggest change in comparison with the previous step is the concentration of compressive stresses on much localized areas in both the left and right on the top of the vault.

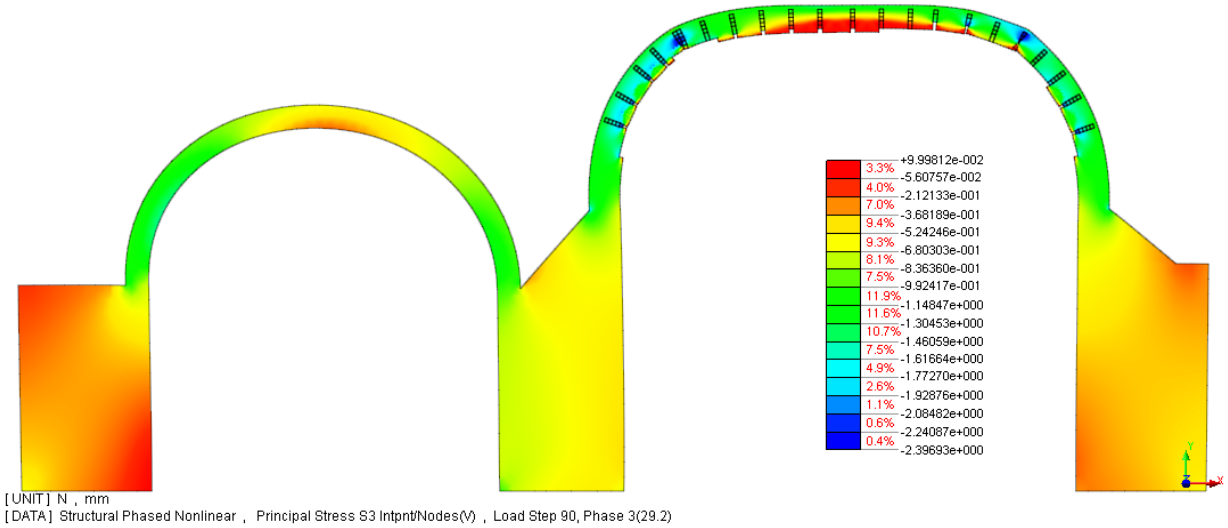

Figure 24. Principal stress σ3 for symmetrical live load Phase 2 at a load factor of 29.2 [MPa]

In the final step the removed elements (Figure 18d) leave a structure that resembles the most the current state of deterioration. A high compressive hinge is clearly formed on the top right of the vault (Figure 25), where crushing of the material would most likely occur. The load factor has decreased from 49 to 23 resulting in a loss of capacity of 53%. Even in these conditions the structure can be considered safe, as the load factor of 23 represents a loading condition of 23 times 5 kN/m^2, which equals to 115k N/m^2.

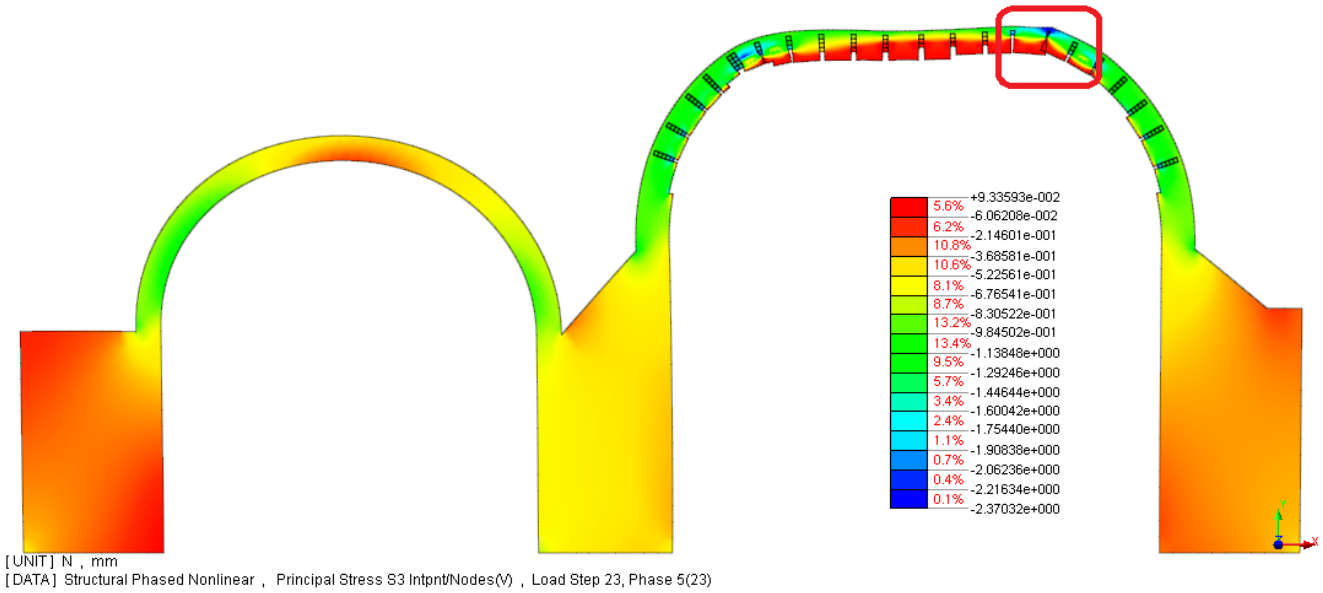

Figure 25. Principal stress S3 for symmetrical live load Phase 3

Figure 26 shows a comparison of the different levels of damage with respect to the original state of the structure. Notice how the increase of damage in the vault results in a loss of stiffness of the structure as the slope of the curve becomes lower each time a group of elements is removed. The load factor shows a significant decrease as a result of the deterioration, original factor for failure due to the increment in the live load factor was 49 and for the Phase 3 this value has been reduced to 23 equivalent to a live load of 115 kN/m^2, less than half the structure original capacity remains.

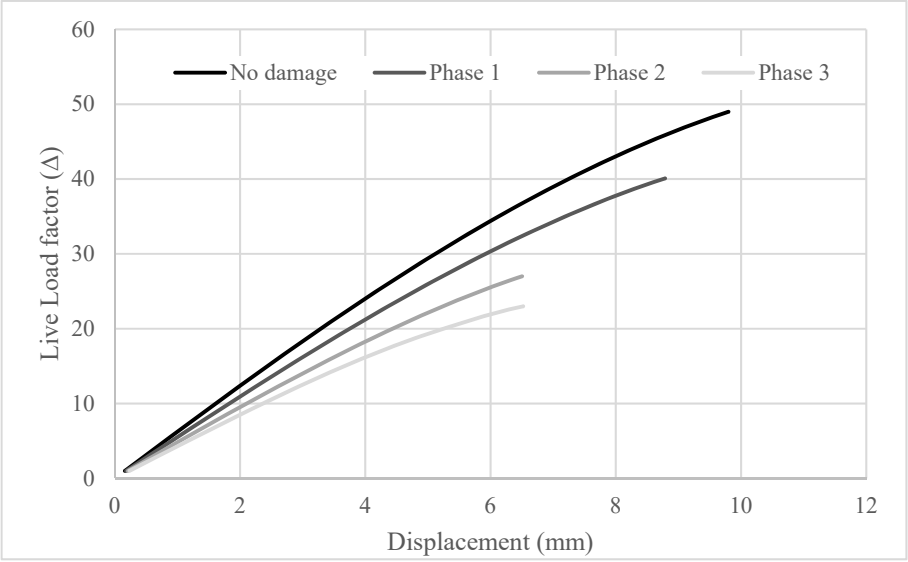

Figure 26. Load vs displacement curves for phased live load analysis.

6 Conclusions

The present paper presents a safety analysis of the San Francisco Master Gate of the Almeida Fortress. The study followed a methodology which included a historic survey, visual inspection, nondestructive testing, and a numerical non-linear analysis, including a sensitivity analysis and phase analysis to simulate the effect of damage in the safety conditions of the gate. For the study, the damage survey played an important role, namely the estimation of the mechanical parameters by sonic testing and the loss of material and morphology of the structure through terrestrial laser scanner and ground penetrating radar.

With the numerical analysis is was possible to conclude that the nonlinear behavior is mainly a consequence of the crushing of the material in compression. Even though cracks develop in the middle of the vault, it is the crushing of the materials in the base of the vault that brings the structure to local failure as a result of the formation of 5 hinges. The sensitivity analysis revealed that in this case the tensile behavior of the masonry does not significant influence the behavior. In contrast, the infill material plays an important role in the response. The phase analysis for live load shows the step by step decrement in the bearing capacity as a consequence of the loss of material where more than 50% of the original capacity seems to be lost. Even in its current damaged state, the ultimate load live factor represents a very high capacity for the structure, since it is a military structure. Although the load factor is still very high and the structure can be considered safe and intervention is advised in order to stabilize the damage process and increase its durability. Further analysis of the structure with 3D elements to simulate the exact shape of the structure, especially the curved vault in plan or micro modelling, will be desirable to compare the response of the different models.

Acknowledgments

The Authors would like to acknowledge the City Council of Almeida for their constant support to promote the studies for promoting the conservation of the Almeida Fortress and to Ing. Carlos Alves Amorim de Barros for his wide and long work in the study of the Almeida Fortress.

This work was financed by FEDER funds through the Competitiveness Factors Operational Programme - COMPETE and by national funds through FCT – Foundation for Science and Technology within the scope of the project POCI-01-0145-FEDER-007633.

References

[1] J. Campos, Almeida, candidatura das fortificações abaluartadas da Raia Luso-Espanhola a patrimonio mundial – UNESCO, Guarda: Camara Municipal de Almeida, 2009.

[2] CEAMA, "Actas das Jornadas da Arquitectura," in *Biannual Magazine of the CEntro de Estudos de Arquitetura Militar de Almeida*, Almeida, 2008.

[3] C. Barros, "Inspeção e diagnóstico das portas magistrais da Fortaleza de Almeida," Universidade do Minho, Braga, 2016.

[4] A. Núñez-García, "Evaluation of structural intervention in the Quartel das Esquadras, Almeida (Portugal)," Universidade do Minho, Braga, 2015.

[5] A. Anzani, L. Binda, A. Carpinteri and G. Lacidogna, "A multilevel approach for the damage assessment of Historic masonry towers," *Journal of Cultural Heritage , Vol. 11,* p. 459–70, 2010.

[6] L. Binda, A. Saisi and C. Tiraboschi, "Application of sonic tests to the diagnosis of damaged and repaired structures," *NDT&E Int, Vol. 34,* p. 123–138, 2001.

[7] ICOMOS, "Recommendations for the analysis, conservation and structural restoration of architectural heritage," International scientific committee for analysis, restoration of structures and architectural heritage, 2005.

[8] I. Lombillo, C. Thomas, L. Villegas, L. Fernández-Álvarez and J. Norambuena-Contreras, "Mechanical char-acterization of rubble stone masonry walls using non and minor destructive tests," *Construction and Build-ing Materials,* vol. 43, pp. 226-277, 2013.

[9] S. Baraccani, S. Silvestri, G. Gasparini, M. Palermo, T. Trombetti, E. Silvestri, R. Lancellotta and A. Capra, "A Structural Analysis of the Modena Cathedral," in *International Journal of Architectural Heritage*, 2015.

[10] Sánchez-Aparicio, L. J., Riveiro, B., Gonzalez-Aguilera, D., & Ramos, L. F., "The combination of geomatic approaches and operational modal analysis to improve calibration of finite element models: A case of study in Saint Torcato Church," *Construction and Building Materials,* pp. 70, 118-129., 2014.

[11] CMA, Candidacy of the bulwarked fortifications of the Portuguese-Spanish "Raia"(Border Line) as world heritage- UNESCO, Almeida, Guarda: Câmara Municipal de Almeida, 2009.

[12] A. L. Quinta, A Fortaleza de Almeida. Uma perspectiva architectonica, Almeida, Portugal: Almeida: Câmara Municipal , 2008.

[13] Sánchez-Aparicio, L. J., Villarino, A., García-Gago, J., & González-Aguilera, D., "Photogrammetric, Geometrical, and Numerical Strategies to Evaluate Initial and Current Conditions in Historical Constructions: A Test Case in the Church of San Lorenzo," *Remote Sensing,* pp. 8(1), 60, 2016.

[14] R. Zlot, M. Bosse, Z. Jarzab, E. Juckes and J. Roberts, "Efficiently capturing large, complex cultural heritage sites with a handheld mobile 3D laser mapping system," *Journal of Cultural Heritage,* pp. 15(6), 670-678, 2014.

[15] Gomes, L., Bellon, O. R. P., & Silva, L., "3D reconstruction methods for digital preservation of cultural heritage: A survey," *Pattern Recognition Letters,* pp. 50, 3-14, 2014.

[16] Besl, P. J., & McKay, N. D., "Method for registration of 3-D shapes," *Paper presented at the Robotics-DL tentative,* 1992.

[17] Toldo, R., Beinat, A., & Crosilla, F., "Global registration of multiple point clouds embedding the Generalized Procrustes Analysis into an ICP framework.," in *Paper presented at the 3DPVT 2010 Conference*, 2010.

[18] Nguyen, V. S., Bac, A., & Daniel, M. , "Simplification of 3D point clouds sampled from elevation surfaces.," 2013.

[19] G. Vasconcelos, P. B. Lourenço, C. A. Alves and J. Pamplona, "Prediction of the mechanical properties of granites by ultrasonic pulse velocity and Schmidt hammer hardness," *Ultrasonics, Vol 48 (5),* pp. 453-466, 2008.

[20] L. Miranda, J. Rio, J. Guedes and A. Costa, "Sonic Impact Method – A new technique for characterization of stone masonry walls," *Construction and Building Materials,* vol. 36, pp. 27-35, 2012.

[21] L. Miranda, J. Guedes, J. Rio and A. Costa, "Stone Masonry Characterization Through Sonic Tests," in *Congreso Internacional sobre Patologia Y recuperacion de Estructuras*, Cordoba, Argentina, 2010.

[22] P. B. Lourenço, "Computational strategies for masonry structures: Multi-scale modelling, dynamics engineering applications and other challenges," in *Congreso de Métodos Numéricos en Ingeniería*, Bilbao, 2013.

[23] P. Lourenço, K. Krakowiak, F. Fernandes and L. Ramos, "Failure analysis of Monastery of Jerónimos, Lisbon: How to learn from sophisticated numerical models," *Engineering Failure Analysis,* vol. 14, no. 2, pp. 280-300, 2007.

[24] L. N. d. E. Civil, "Norma Portuguesa: Eurocódigo 8: Projecto de estruturas para resistência aos sismos," Instituto Português da Qualidade, Caparica, 2009.

[25] DIANA, "DIANA FEA BV 9.6 [computer software]," 2014a.

[26] MIDAS, "Midas FX+ [computer software], MIDAS Information Technology Co., Ldt," 2015.

[27] DIANA, DIANA User's Manual Release 9.6, J. M. a. W. P. Kikstra, Ed., Delft: TNO DIANA bv, 2014b.

[28] I. Garcia-Roca, "Safety Evaluation of the Imperfect Chapels from Batalha Monastery," MSc Thesis, University of Minho, Guimarães, Portugal, 2015.

[29] P. Lança, P. B. Lourenço and G. Bahman, "Structural assessment of a masonry vault in Portugal," *Proceedings of the Institution of Civil Engineers - Structures and Buildings,* vol. 168, no. 12, pp. 915-929, 2015.

[30] European commission, "Winners of 2012 EU Prize for Cultural Heritage / Europa Nostra Awards announced," 11 November 2016. [Online]. Available: http://europa.eu/rapid/press-release_IP-12-254_en.htm?locale=en.

[31] Quagliarini, E., Clini, P., & Ripanti, M., "Fast, low cost and safe methodology for the assessment of the state of conservation of historical buildings from 3D laser scanning: The case study of Santa Maria in Portonovo," *Journal of Cultural Heritage,* 2016.

[32] Toldo, R., Beinat, A., & Crosilla, F., "The integration of geotechnologies in the evaluation of a wine cellar structure through the Finite Element Method," *Remote Sensing,* pp. 6(11), 11107-11126, 2014.

[33] P. Rodríguez-Gonzálvez, Á. Muñoz-Nieto, I. Gozalo-Sanz, J. Mancera-Taboada, D. González-Aguilera and P. Carrasco-Morillo, "eomatics and Geophysics Synergies to Evaluate Underground Wine Cellars," in *International Journal of Architectural Heritage*, 2014.